Electrocapillary at Contact: Potential-Dependent Adhesion between a Gold Electrode and a Mica Surface

Joëlle Fréchette and T. Kyle Vanderlick*

Department of Chemical Engineering, Princeton University, Princeton, New Jersey 08540

Received September 8, 2004. In Final Form: October 26, 2004

Using the electrochemical surface forces apparatus, we investigated adhesion (from pull-off measurements) between gold and mica as the potential of the gold surface was changed externally. Measurements were performed at different concentrations of $KClO_4$ in a potential window where the gold electrode is ideally polarizable. At applied potentials where the gold−mica interactions are repulsive, we obtain double layer forces that are predictable by the Derjaguin−Landau−Verwey−Overbeek (DLVO) theory of colloid stability but deviate from the theory at short range. At applied potentials where the gold−mica interactions are attractive, we observed a very strong dependence of adhesion on the applied potential, a result that cannot be directly related to DLVO theory. We show, however, that an approach based on electrocapillary thermodynamics can be employed to model the potential dependence of adhesion seen in our measurements. This electrocapillary approach presents evidence of charging at the gold−mica interface and stresses the relation between the charge within and outside of the contact area.

Introduction

The need to actively control interfacial properties is gaining importance with the development of new devices relying on the external actuation of adhesion, wetting, and spreading.[1] The ideal device would allow for external, real-time, and reversible control of such events through the change of, for example, electric potential, electrical field, or illumination. Microelectromechanical systems (MEMS) designed to operate in liquids[2] are an example of a technology that would greatly benefit from a better understanding of how the properties of a solid−liquid interface can be altered externally. Surface forces in liquids can be quite different from those in air, because factors such as the presence of diffuse ionic double layers or hydrogen bonding can come into play. Ideally, one would like to manipulate forces to control the interactions between two surfaces in a liquid environment, including the scenario of creating adhesive contact.

One way to actively and reversibly control adhesion between surfaces in liquids is to apply an external potential to one or both of the surfaces. This applied potential can induce a chemical reaction, cause dissociation of surface endgroups,[3] or align an adsorbate.[4,5] All of these effects can, in turn, change the contact behavior between surfaces with the added advantage of being reversible and externally controlled.

Adhesion measurements themselves can serve as an analytical tool to characterize the chemical nature of a surface. Such measurements have been used to map the presence of different endgroups on a surface and to probe the dissociation state of a monolayer as the pH or electric potential is changed.[6−8] It has been shown that the pK_a of a dissociable endgroup is different when the group is attached on a surface than when it is dissolved in solution.[9] Also, the oxidation/reduction state of a surface produces noticeable changes in its contact properties.[10] A difficulty in using adhesion measurements as a surface characterization tool is that one cannot necessarily deconvolute different surface transformations that may occur. For example, a change in applied potential on an electrode covered with a monolayer may cause a variation in the surface potential and simultaneously some level of dissociation of the monolayer; these effects cannot easily be separated experimentally.

The advent of the atomic force microscope,[11] modified to measure forces in liquid,[12,13] has stimulated a host of studies on adhesion in liquid environments. For example, Smith et al.[8] measured adhesion between silica and two surfaces (each coated with a different dissociable self-assembled monolayer) as a function of pH at different salt concentrations. They observed stronger adhesion and a loss of the typical sigmoidal dependence of adhesion on pH at low salt concentration. Serafin et al.[14] studied the impact of underpotential deposition on adhesion between a gold electrode and a Si_3N_4 tip. They also investigated the adhesion between gold and silicon nitride in basic environments as a function of applied potential and estimated a value for the hydrogen bonding energy generated by the adsorption of AuOH at high applied potentials.[15] Raiteri et al.[16] measured double layer forces as well as adhesion between metals (gold or platinum) and a silicon nitride tip. Working in an electrochemical

* To whom correspondence should be addressed. Phone: (609) 258-4891. Fax: (609) 258-0211. E-mail: vandertk@princeton.edu.

(1) Rosslee, C.; Abbott, N. L. *Curr. Opin. Colloid Interface Sci.* **2000**, *5*, 81.
(2) Lee, J.; Kim, C. J. *J. Microelectromech. Syst.* **2000**, *9*, 171.
(3) Smith, C. P.; White, H. S. *Anal. Chem.* **1992**, *64*, 2398.
(4) Stolberg, L.; Richer, J.; Lipkowski, J.; Irish, D. E. *J. Electroanal. Chem.* **1986**, *207*, 213.
(5) Poortinga, A. T.; Smit, J.; van der Mei, H. C.; Busscher, H. J. *Biotechnol. Bioeng.* **2001**, *76*, 395.
(6) Vezenov, D. V.; Noy, A.; Rozsnyai, L. F.; Lieber, C. M. *J. Am. Chem. Soc.* **1997**, *119*, 2006.
(7) Schneider, J.; Berndt, P.; Haverstick, K.; Kumar, S.; Chiruvolu, S.; Tirrell, M. *Langmuir* **2002**, *18*, 3923.
(8) Smith, D. A.; Wallwork, M. L.; Zhang, J.; Kirkham, J.; Robinson, C.; Marsh, A.; Wong, M. *J. Phys. Chem. B* **2000**, *104*, 8862.
(9) Hu, K.; Bard, A. J. *Langmuir* **1997**, *13*, 5114.
(10) Green, J.-B. D.; McDermott, M. T.; Porter, M. D. *J. Phys. Chem.* **1996**, *100*, 13342.
(11) Binnig, G.; Quate, C. F.; Gerber, C. *Phys. Rev. Lett.* **1986**, *56*, 930.
(12) Ducker, W.; Senden, T. J.; Pashley, R. M. *Nature* **1991**, *353*, 239.
(13) Ducker, W. A.; Senden, T. *Langmuir* **1992**, *8*, 1831.
(14) Serafin, J. M.; Hsieh, S.-J.; Monahan, J.; Gewirth, A. A. *J. Phys. Chem. B* **1998**, *102*, 10027.
(15) Serafin, J. M.; Gewirth, A. A. *J. Phys. Chem. B* **1997**, *101*, 10833.
(16) Raiteri, R.; Grattarola, M.; Butt, H.-J. *J. Phys. Chem.* **1996**, *100*, 16700.

10.1021/la047750x CCC: $30.25
Published on Web 01/05/2005

environment allowed them to attain a large range of surface forces over a small applied potential window; however, uncertainties regarding the geometry of the system prevented analytic comparison of the effect of applied potential on adhesion. All these experiments highlight the interplay of electrostatic, van der Waals, and hydrogen bonding forces. Notably, there has been limited work where charging of a surface was not combined with chemical changes such as dissociation or surface deposition.

In this work, we studied adhesion between gold and mica as the potential of the gold surface is changed externally. We focused our work on a potential region where the gold electrode is ideally polarizable (no current flow) such that the adhesion measured as a function of applied potential originated solely from charging rather than being combined with other chemical effects such as electrochemical reaction or dissociation. We observed a very strong dependence of adhesion on the applied potential when the noncontact interactions between the gold and mica are attractive. These measurements, although electrostatic in nature, can hardly be predicted using simple Derjaguin−Landau−Verwey−Overbeek (DLVO) theory. We put forward an approach based on the concept of electrocapillary thermodynamics to model our potential-dependent adhesion measurements. This electrocapillary approach shows evidence of charging at the gold−mica interface and highlights the interplay between the different interfaces in the system (i.e., gold−mica, gold−solution, and mica−solution).

Experimental Section

Electrochemical Surface Forces Apparatus (ESFA). The ESFA[17] is a modified version of the original surface forces apparatus (SFA) developed over 30 years ago[18] allowing potential control of one or both of the surfaces studied. The key modification is the substitution of uniquely fabricated electrodes for the mica substrates commonly used in the apparatus. Briefly, electrodes for use in the ESFA are made by gluing a clean, molecularly smooth piece of mica to the standard silica disk employed in the SFA. The mica piece is then treated with oxygen plasma and masked by another, smaller, mica piece, which remains held by van der Waals forces. Next an adhesive layer of titanium (ca. 15 nm) is evaporated on the mica followed immediately by a thick (ca. 150 nm) layer of gold. Pure indium is then used to solder a fine gold wire at the extreme corner of the gold-covered mica sheet and a layer of epoxy subsequently covers the connection. Finally, the masking mica piece is removed and final thin layers of titanium (ca 1.5 nm) and gold (ca. 60 nm) are evaporated creating a gold region at the center of the substrate, thin enough for effective employment of multiple beam interferometry. The electrode is used immediately in the SFA.

Beyond electrode preparation, having potential control inside the SFA requires additional considerations. We use a Teflon bath for the electrolyte instead of filling the whole chamber. The gold electrode described above is connected to a potentiostat (PAR 263A, Oak Ridge, TN) as a working electrode and a gold gauze (82 mesh, 99.9%, Alfa, Ward Hill, MA) is placed inside the Teflon bath as a counter electrode. The reference electrode is a palladium pseudo-reference electrode[19] or a Ag/Ag_2S wire.[20] The potential of the gold electrode (measured with respect to the Pd/H_2 or Ag/Ag_2S quasi-reference) is translated to a Ag/AgCl(3M) (Brinkmann, Westbury, NY) scale by measuring the open circuit potential difference between the two references at the end of each experiment. Forces and adhesion measurements are performed within the double layer potential window (i.e., where the gold electrode can be considered ideally polarized) as determined by cyclic voltammetry.

There are two major issues regarding the measurements of surface separation in the ESFA: the nature of the optical filter (titanium/gold/solution/mica/silver) and the roughness of the gold surface. The unsymmetrical nature of the optical filter prevents one from using simple analytical expressions based on the reference case of zero surface separation.[21] Instead, the multi-matrix method[22,23] must be employed and this requires that the thicknesses of the mica be explicitly known. The mica thickness is determined by interferometry using pieces of thickness equivalent to that used in the ESFA. The roughness of the gold surface is taken into account in the interferometric analysis of the surface separation by modeling the rough gold substrate as a two-layer system composed of a smooth gold substrate with a uniform dielectric overcoat of thickness on the order of the root mean square (RMS) of the gold (we have previously referred to this overcoat as a "residual dielectric gap").[24] The gold surface was characterized using atomic force microscopy (AFM) as being polycrystalline with a preference for (111) orientation and as having a RMS of 3 nm.[25,26] The values we determined for the residual dielectric gap varied between 40 and 60 Å for each experiment, consistent with the RMS measured independently using AFM. During force measurements, the separation is inferred from the increase in the dielectric thickness beyond that which accounts for the residual dielectric gap.

Materials. Solutions of $KClO_4$ (0.1mM to 10mM) were prepared from highest available purity salts (99.99%, Aldrich, Miliwaukee,WI) which were used without further purification and dissolved in 18.2 MΩ deionized water (Hydro Services, Levittown, PA). The solutions were unbuffered and had a pH of about 5.5. The gold working electrode was made by thermal evaporation (ca. 2.0 Å/s) using high-purity gold (99.999%, Cerac, Miliwaukee, WI) and titanium (99.99%, Alfa). The solder was high-purity indium (99.999%, Cerac) and covered with epoxy (Hysol, 0151, Dexter, CA). Mica sheets (Ruby, ASTM V-2, S&J Trading, NY) were cleaved in a laminar hood and put on a larger mica backing sheet. This backing sheet was then coated with a silver film (99.999%, Alfa) approximately 48-nm thick (formed at a rate of 3.5 Å/s). Mica substrates for use in the ESFA were created by peeling a small mica sheet off the backing plate and gluing it silver-side down onto a silica disk with a thermoset epoxy (Shell, Epon 1004).

Procedure. The cleaning procedure undertaken before every experiment has been described previously.[17] The final evaporation for the electrode was carried out just before the experiment, and the electrode was brought directly from the vacuum chamber (5×10^{-8} Torr) to the clean room for assembly in the SFA. Once the apparatus was completely assembled with all electrical connections in place, gold and mica were brought into contact in air and the fringe positions were recorded. In all experiments, the initial contact with mica was strongly adhesive ensuring a level of cleanliness of the electrode. We cannot, however, rule out some minimal level of surface contamination. The surfaces were then separated, and the solution was injected using a reagent bottle pressurized with humid nitrogen and equipped with all Teflon tubing and valves (Omnifit, Rockville Center, NY). The solution was deaerated with humid nitrogen for 30 min before use, and the experiment was done under a slight positive pressure of nitrogen. The solution was left in the apparatus for 1−2 h to allow for temperature equilibration.

The potential of the gold electrode was controlled with a potentiostat. Cyclic voltammetry was carried out to identify the double layer region and to remove possible impurities from the gold surface. The double layer region was found to be between −0.35 to +0.55 V. The current was also monitored throughout the experiment to ensure that there was little faradic current.

(17) Fréchette, J.; Vanderlick, T. K. *Langmuir* **2001**, *17*, 7620.
(18) Tabor, D.; Winterton, R. H. S. *Proc. R. Soc. London, Ser. A* **1969**, *312*, 435.
(19) Fleischmann, M.; Hiddleston, J. N. *J. Sci. Instrum.* **1968**, *1*, 667.
(20) Ives, D. J. G.; Janz, G. J. *Reference electrodes, theory and practice*; Academic Press: New York, 1961.
(21) Israelachvili, J. N. *J. Colloid Interface Sci.* **1973**, *44*, 259.
(22) Clarkson, M. T. *J. Phys. D: Appl. Phys.* **1989**, *22*, 475.
(23) Levins, J. M.; Vanderlick, T. K. *Langmuir* **1994**, *10*, 2389.
(24) Levins, J. M.; Vanderlick, T. K. *J. Colloid Interface Sci.* **1993**, *158*, 223.
(25) Knarr, R.; Quon, R. A.; Vanderlick, T. K. *Langmuir* **1998**, *14*, 6414.
(26) Levins, J. M.; Vanderlick, T. K. *J. Colloid Interface Sci.* **1997**, *185*, 449.

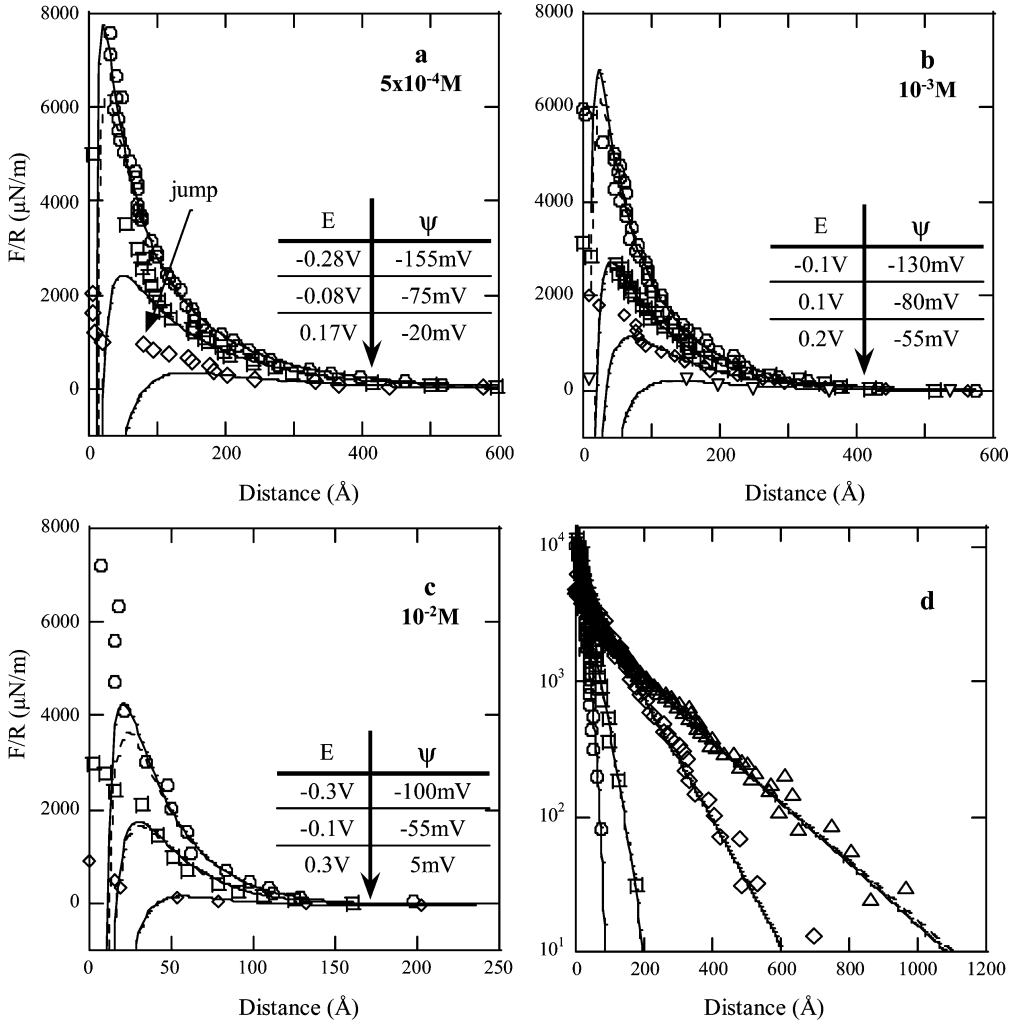

Figure 1. Measured and theoretical forces (normalized by the radius of curvature). Parts a−c are forces between gold and mica, part d is a series of forces between two mica surfaces in 3×10^{-4} M ($\Psi^{\infty} = -125$ mV), 10^{-3} M ($\Psi^{\infty} = -130$ mV), 10^{-2} M ($\Psi^{\infty} = -82$ mV), and 5×10^{-2} M ($\Psi^{\infty} = -90$ mV). The Hamaker constant for gold−mica is 8.4×10^{-20} J, and the Hamaker constant for mica−mica 2.2×10^{-20} J. The table inset in each graph shows the relationship between the applied potential and the fitted potentials, and the mica surface potential used for the gold−mica DLVO fits is the one obtained from the mica−mica forces. The applied potential is expressed on the Ag/AgCl(3M) scale.

A charge-coupled device camera (Photometrics, Tucson, AZ) was used to determine the positions of interference fringes from which pull-off separations, as well as the mean radius of curvature of the interacting substrates, were calculated. The fringe positions yielding the separation dependence of the double layer forces were recorded manually. For experiments involving two mica surfaces, the same procedure was followed without the use of electrodes. All experiments were performed at 22 °C in a controlled temperature environment.

Results

The investigation of adhesion between the gold electrode and the mica surface is well-complemented by characterizing the governing noncontact interactions, namely, the double layer forces which act over a long range. Studying these forces allows for a better understanding of the charging behavior of a surface. In particular, double layer interactions are very suitable for comparison with DLVO theory and yield parameters such as the surface potential, the Debye length, and the potential of zero force (PZF). These measurements extend the pool of data available in the literature and act as a useful checkpoint of the experimental conditions. More importantly, determination of the PZF is central to our analysis of adhesion measurements as it is used as a direct input in our electrocapillary model. In addition, measurements of deviations from traditional double layer theory could be used for testing more complex models of the electrified interfaces which might take into account factors such as the structure of confined liquids and the forces caused by hydration and adsorption on the surface.

We, thus, divide our results in two parts: double layer force measurements and attractive pull-off data. Although both measurements are obtained as part of a single experiment, the approach in analyzing the data is different. Force measurements were made in different concentrations of $KClO_4$ solutions. $KClO_4$ was chosen both because it is well established that perchlorate ions do not specifically adsorb at the gold surface and also because the electrochemical behavior of the gold electrode in this electrolyte is well-characterized.[27]

Double Layer Interactions. Shown in Figure 1a−c are the repulsive double layer forces between mica and gold held at different applied potentials, as measured in three different salt concentrations (5×10^{-4} M, 1×10^{-3} M, and 10^{-2} M $KClO_4$). Figure 1d shows the double layer forces measured between two mica sheets in the same solutions, which yield the surface potential of the mica at

(27) Clavilier, J.; Nguyen Van Huong, C. *J. Electroanal. Chem.* **1977**, *80*, 101.

each $KClO_4$ concentration. Also presented in Figure 1 are predictions from DLVO[28,29] theory obtained by solving numerically the Poisson−Boltzmann equation. The two fitting lines correspond to the limiting cases for the charging behavior of the mica surface, namely, constant charge and constant potential. Because it is a conductor, the gold surface is assumed to be at a constant potential. Only one fitting parameter is used to match theory with experiment. In the mica−mica experiments, that parameter is the surface potential of the mica at infinite surface separation. In the gold−mica experiments the value of the gold surface potential was used to fit the data. Other variables input to the theory were obtained as follows. The strength of the van der Waals interaction was calculated using a Hamaker constant (nonretarded case) of 2.2×10^{-20} J[30] in the case of mica−mica interactions and a value of 8.4×10^{-20} J[31,32] for the gold−mica interactions (obtained by a geometric averaging of literature values for gold and mica). The injected solution concentration was used to calculate the Debye length. As is seen in Figure 1, the Debye length observed corresponds well to the prediction based on the concentration in solution for all cases where repulsive forces are measured.

As is readily seen, forces correspond well to predictions at separations larger than the Debye length. Some significant deviations, however, are observed at shorter separations. At high negative applied potential, the forces are purely repulsive (no hysteresis between the approach and retraction curves) showing no evidence of van der Waals forces (e.g., see the upper curve in Figure 1a). (Similar non-DLVO forces have often been observed at short range in many other force measurements, and the origin of short-range double layer forces is a matter of debate; see the work of Shubin and Kekicheff,[33] for example.) As the applied potential becomes more positive, the surfaces jump into contact. This jump (during which no approach curve can be measured) occurs when the gradient of the force is greater than the spring constant resulting in instability of the spring (e.g., see the lower curve in Figure 1a). At sufficiently positive potentials, the forces become purely attractive; that is, the surfaces jump into contact before any forces can be measured.

We previously reported the large range of potentials achievable with this technique.[17] Figure 1 shows that the same range of potentials can be obtained independent of the salt concentration. At high negative potentials, repulsive forces often reach a regime where a change in applied potential has little effect on the measured forces because of a force saturation effect. This is notable because gold is known to be amphifunctional,[34−37] where the charge on the surface is not solely a function of the applied potential but also a function of pH. The relatively low surface potentials obtained from double layer force

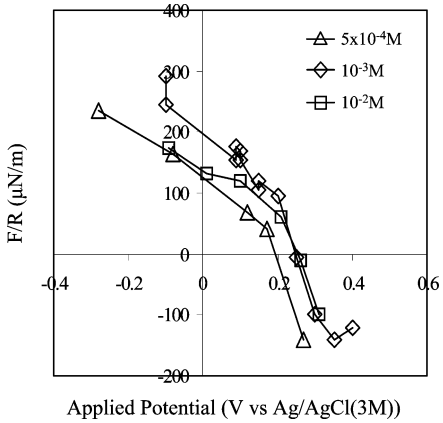

Figure 2. Measured forces between gold and mica at different applied potentials at a fixed separation. For 5×10^{-4} M the value of the force at 400 Å is plotted, and for 10^{-3} M the value of the force measured at 300 Å and for 10^{-2} M the value of the force measured at 120 Å are shown. The PZF is determined as the applied potential at which the measured force is zero.

measurements between a gold electrode and a silica surface have been taken, by other investigators,[37] as evidence of this dual charging processes of gold. The surface charge dependence on pH is caused by adsorption of amphoteric hydroxyl surface groups from solution, creating acid/base sites on the gold surface (site density estimated to be around 10^{12} sites/cm^2, roughly 0.1% coverage).[36] This adsorption can have two main effects: reducing the impact of applied potential on the surface potential (reducing the range of surface potential attainable) and moving the PZF to higher values as the pH passes the isoelectric point (iep = 4.95). The large range of surface potentials we observe indicates that the gold surface under study behaves primarily as a conductor and is not significantly amphifunctional. We cannot rule out, however, the possibility of some charge regulation due to adsorption and partial discharge of hydroxyl groups.

Using the approach of Hillier et al.,[31] we determined the PZF from our double layer force measurements. We define the PZF as the potential for which no forces are measured. More explicitly, we take the value of the measured force for a large separation to avoid the onset of van der Waals forces and to get only a small compression of the interacting double layers. Minimizing the double layer overlap also permits the determined PZF value to correspond to the applied potential for which the gold surface potential is zero (because forces between a charged surface and an uncharged wall will be measurable when the double layer of the charged surface is compressed). The separations chosen to extract the PZF are between 120 and 400 Å depending on the salt concentration. Previous researchers[31,38] have shown that the PZF is equivalent to the more commonly used potential of zero charge (PZC, obtained from differential capacitance data). Figure 2 shows the PZF obtained in three different solutions, showing a slight variation with salt concentration but remaining between 0.2 and 0.25 V versus Ag/AgCl. This value is higher than some commonly accepted results measured for similar surfaces[27] but does correspond well to what was obtained by Wang and Bard[38] and Barten et al.[37] for a pH of about 5.5 measured using differential capacitance and surface forces. Barten et al. suggested that a solution at a pH higher than the gold iep (4.95) would cause the PZF to move to more positive values (as we observed) because of adsorption of amphoteric hydroxyl surface groups.

(28) Derjaguin, B. V.; Landau, L. *Acta Physicochim. URSS* **1941**, *14*, 633.
(29) Verway, E. J. W.; Overbeek, J. T. *Theory of Stability of Lyophobic Colloids*; Elsevier: New York, 1948.
(30) Israelachvili, J. N.; Adams, G. E. *J. Chem. Soc., Faraday Trans. 1* **1978**, *74*, 975.
(31) Hillier, A. C.; Kim, S.; Bard, A. J. *J. Phys. Chem.* **1996**, *100*, 18808.
(32) Biggs, S.; Mulvaney, P. *J. Chem. Phys.* **1994**, *100*, 8501.
(33) Shubin, V. E.; Kekicheff, P. *J. Colloid Interface Sci.* **1993**, *155*, 108.
(34) Thompson, D. W.; Collins, I. R. *J. Colloid Interface Sci.* **1992**, *152*, 197.
(35) Giesbers, M.; Kleijn, J. M.; Stuart, M. A. C. *J. Colloid Interface Sci.* **2002**, *248*, 88.
(36) Duval, J.; Lyklema, J.; Kleijn, J. M.; van Leeuwen, H. P. *Langmuir* **2001**, *17*, 7573.
(37) Barten, D.; Kleijn, J. M.; Duval, J.; von Leeuwen, H. P.; Lyklema, J.; Stuart, M. A. C. *Langmuir* **2003**, *19*, 1133.
(38) Wang, J.; Bard, A. J. *J. Phys. Chem. B* **2001**, *105*, 5217.

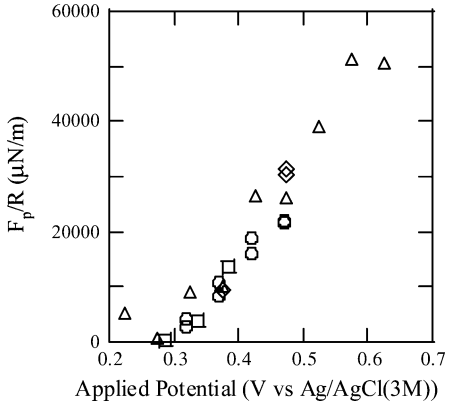

Figure 3. Pull-off forces (normalized by the radius of curvature) measured as a function of applied potential [vs Ag/AgCl(3M)] in 10^{-3} M $KClO_4$. Different symbols correspond to different experiments (different surfaces and solutions).

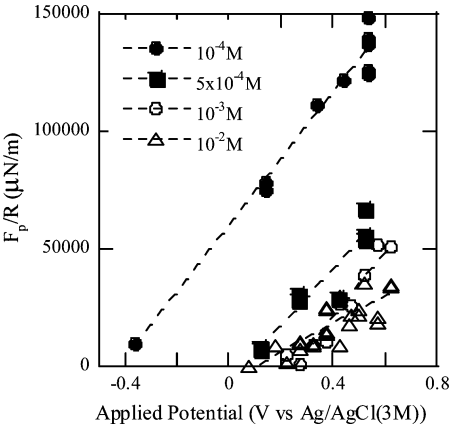

Figure 4. Pull-off forces (normalized with the radius of curvature) as a function of applied potential for all four concentrations of $KClO_4$ (10^{-4}, 5×10^{-4}, 10^{-3}, and 10^{-2} M). The lines are to guide the eye.

Adhesion. Figure 3 shows the value of the pull-off forces as a function of applied potential in 10^{-3} M $KClO_4$. The different symbols correspond to independent experiments (different surfaces and solutions) showing the high reproducibility of the adhesion measurements from experiment to experiment. It is important to note that pull-off measurements were not taken in order of increasing potential; effort was made to go back and forth between different values. Two features of these adhesion measurements stand out. First, the interaction increases dramatically over a 0.3-V window. Second, the great majority of these attractive forces are stronger (in absolute value) than the largest repulsive force measured at the highest applied negative potential.

Figure 4 compares the pull-off forces measured across all four salt concentrations studied. As noted by other investigators,[8] lower salt concentration greatly increases the adhesion between the two surfaces, with much of the concentration effect happening below 10^{-3} M. In addition, we also observe that the adhesion measurements follow a similar potential dependence between 10^{-4} and 10^{-3} M but the measured pull-off forces at higher concentration are shifted to potentials that are more positive.

Discussion

DLVO theory does not arm us with a direct framework for understanding forces between bodies in contact, so we also seek a theoretical platform (ideally, a simple one) that might be applied to interpret these measurements. As will be shown, the well-known electrocapillary approach used to understand liquid−liquid interfaces can be extended to the situation at hand. To do so, however, first requires a brief discussion on relating pull-off forces to the thermodynamic concept of work of adhesion. We, thus, divide our discussion into three segments. In the first, we show that it is reasonable to employ Johnson−Kendall−Roberts (JKR) theory of contact mechanics to obtain works of adhesion from the measured pull-off forces. In the second part, we present the electrocapillary approach. In the third part, we apply this approach to the systems studied herein.

Determination of the Work of Adhesion. According to the JKR theory of contact mechanics,[39] the pull-off force is related to the work of adhesion between two surfaces by

$$\frac{F_p}{R} = \frac{3\pi}{2} W_{ADH} \tag{1}$$

At the root of JKR theory is the assumption that substrates interact only across the area of contact. Muller et al.[40,41] established a dimensionless parameter to test the validity of JKR theory for a given system by comparing the relative importance of all the parameters characteristic of the system:

$$\mu = \frac{64}{3\pi}\left[\frac{W^2 R}{4\pi K^2 D_0^{\,3}}\right]^{1/3} \tag{2}$$

Here, W is the work of adhesion, R is the effective radius of curvature, K is the effective modulus of the system, and D_0 represents the closest approach between the surfaces. For JKR theory to be valid, the parameter μ should be greater than unity. A value of μ less than unity signifies that interactions out of the contact area are important, and, thus, the Derjaguin−Muller−Toporov theory[42] would apply. In our experiments, the modulus can be estimated to be about 20 GPa,[25] R is always between 1 and 2 cm, and we estimate a minimum separation between gold and mica of 2 Å. We, thus, obtain values of μ between 2 and 50 (average of 14) justifying the use of JKR theory to convert pull-off force measurements to values of work of adhesion. This simplifies the analysis of the pull-off data because we can neglect contributions coming from out of the area of contact.

Understanding Solid−Solid Contact Using an Electrocapillary Approach. The work of adhesion in our system can be expressed as

$$W_{ADH} = \gamma_{GL} + \gamma_{ML} - \gamma_{GM} \tag{3}$$

where γ_{GL} represents the surface energy (energy per unit area) of the gold−liquid interface, γ_{ML} is the surface energy of the mica−liquid interface, and γ_{GM} represents the surface energy of the gold−mica interface. The dependence of the work of adhesion on applied potential is, thus, directly related to the dependence of these various surface energies on the applied potential.

In a potential region where the gold−liquid interface is ideally polarized (i.e., when there is no charge transfer),

(39) Johnson, K. L.; Kendall, K.; Roberts, A. D. *Proc. R. Soc. London, Ser. A* **1971**, *324*, 301.
(40) Maugis, D. *J. Colloid Interface Sci.* **1992**, *150*, 243.
(41) Muller, V. M.; Yushchenko, V. S.; Derjaguin, B. V. *J. Colloid Interface Sci.* **1980**, *77*, 91.
(42) Derjaguin, B. V.; Muller, V. M.; Toporov, Y. P. *J. Colloid Interface Sci.* **1975**, *53*, 314.

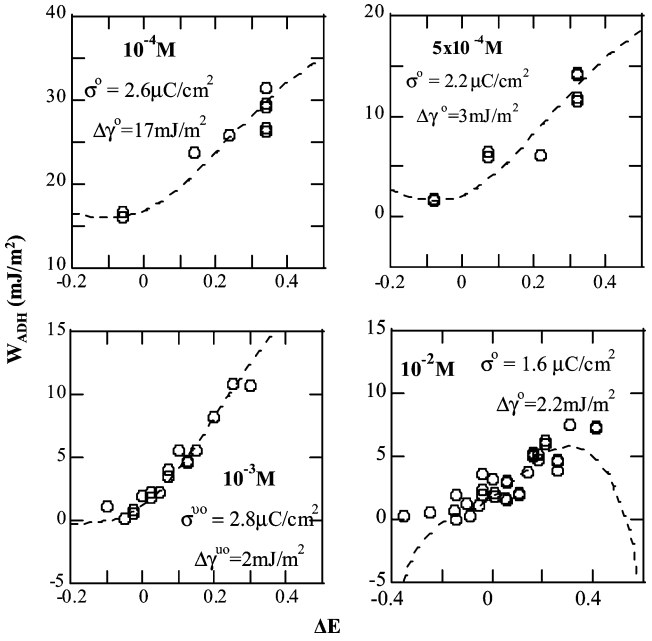

Figure 5. Measured and predicted value of the work of adhesion (W_{ADH}) as a function of applied potential. The work of adhesion was obtained from the pull-off measurements using JKR theory, and the applied potential was translated with the PZF. The predicted values were obtained with a capacitance of the gold−mica interface of 30 μF/cm^2 (ref 45) and published data[27] for the charging behavior of the gold−liquid interface. The predicted values are expressed as translated with the PZC of the gold−liquid interface (E^{GL}_{PZC}).

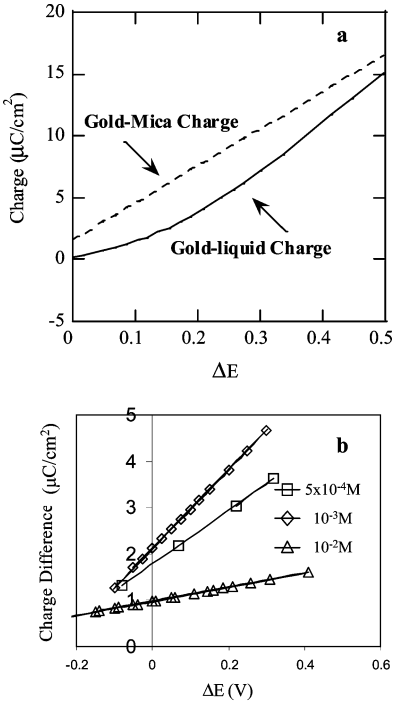

Figure 6. (a) Value of the calculated charge at the gold−mica and gold−liquid interfaces as a function of the applied potential (corrected with the PZC of the gold−liquid interface) for 10^{-3} M $KClO_4$. (b) Charge difference between the gold−mica and the gold−liquid interface shifted with the PZF as a function of applied potential obtained directly from the pull-off measurements (no fitting parameters).

the surface energy, surface charge, and applied potential are related by the Lippmann equation:[43]

$$\sigma_{GL} = -\left(\frac{\partial \gamma_{GL}}{\partial E}\right)_{P,T,n_i} \quad (4)$$

where σ_{GL} is the charge density at the gold−liquid interface, E is the applied potential, P is the pressure, T is the temperature, and n_i is the solution composition. This is the electrocapillary equation used extensively by Grahame[44] for the mercury−solution interface. The surface energy reaches a maximum when the surface is not charged at the PZC and decreases as the potential moves away (positively or negatively) from the PZC, following an inverted parabolic shape.

Equations 3 and 4 predict that if γ_{GL} is the only surface energy term to depend on the applied potential, the pull-off forces would actually decrease as the gold surface becomes more positively charged, which is clearly not what we observed in this work. Mica is a good insulator; it can be assumed that its surface energy (γ_{ML}) is independent of the gold potential. Therefore, γ_{GM} not only has to depend on the applied potential but also must decrease at a faster rate than the gold−liquid interface for the work of adhesion to increase as the potential increases. For the gold−mica interface to have such potential dependence, a charge separation must be established at the gold−mica interface, which can be described using the Lippmann equation (if we assume this form of the electrocapillary equation is valid for a solid−solid interface). This is a similar view to the one presented by Horn[45] in their investigation of the potential dependence of the contact angle of mercury on a mica surface.

An analytical expression for the gold−mica surface energy (as a function of applied potential) can be derived from the Lippmann equation. For simplicity of further analysis, we express the applied potential axis as a departure from the gold−liquid PZC ($E = 0$ for $E = E^{GL}_{PZC}$). Therefore, the surface energy of the gold−mica interface can be given by

$$\gamma_{GM} = -C_{GM}(E - E^{GL}_{PZC})^2 - \sigma_0(E - E^{GL}_{PZC}) + \gamma^0_{GM} \quad (5)$$

where C_{GM} is the capacitance at the gold−mica interface, E is the applied potential, E^{GL}_{PZC} is the PZC of the gold−liquid interface, σ_0 is the charge at the gold−mica interface at the E^{GL}_{PZC}, and γ^0_{GM} is the surface energy of the gold−mica at the E^{GL}_{PZC}. A direct consequence of charge separation at the gold−mica interface is that its charge is nonzero at the E^{GL}_{PZC} (the gold−mica interface has its own PZC). This is because gold is a metal and, therefore, an equipotential material; the charge can follow a nonuniform distribution and, in fact, must do so to keep the local potential constant. Thus, the potential dependence predicted by the Lippmann equation for the gold−liquid and the gold−mica interfaces need not be the same.

The work of adhesion can then be expressed as

$$W_{ADH} = \gamma_{GL}[\text{function of } (E - E^{GL}_{PZC})] + \gamma_{ML} - \gamma_{GM}[\text{function of } (E - E^{GL}_{PZC})] \quad (6)$$

and more formally as

(43) Bard, A.; Faulkner, L. R. *Electrochemical Methods Fundamentals and Applications*; John Wiley & Sons: New York, 1980.
(44) Grahame, D. C. *Chem. Rev.* **1947**, *41*, 441.
(45) Antelmi, D. A.; Connor, J. N.; Horn, R. G. *J. Phys. Chem. B* **2004**, *108*, 1030.

$$W_{ADH} = -\int\int C_{GL}\, dE + [C_{GM}(E - E_{PZC}^{GL})^2 + \sigma_{GM}^0(E - E_{PZC}^{GL})] + (\gamma_{GL}^0 + \gamma_{ML}^0 - \gamma_{GM}^0) \quad (7)$$

This is a powerful result and provides a framework for analyzing the potential dependence of adhesive forces. In particular, this equation provides a route to connect force data with two basic physical characteristics of the system: (1) σ_{GM}^0, which represents the charge at the gold−mica interface at the E_{PZC}^{GL}, and (2) $\Delta\gamma^0 = (\gamma_{GL}^0 + \gamma_{ML}^0 - \gamma_{GM}^0)$, which represents the work of adhesion at the E_{PZC}^{GL}. This connection is possible because other pieces of eq 7 can be readily approximated or can be independently measured.

One can make, for example, a reasonable estimate for the capacitance of the gold−mica interface using the same arguments as put forward by Horn and co-workers for the capacitance of a mercury−mica interface. A value of 0.3 F/m^2 is reasonable (obtained by assuming intimate contact and the position of the charged group on the mica surface to be localized within 2 Å of the mica). Meanwhile, the differential capacitance for the gold−liquid interface could be obtained (using AC voltammetry, for example) during the experiment, or the charge density at the gold−liquid interface could be directly measured by chronocoulometry (which we did not attempt in this work); however, in lieu of direct measurements such data is readily available in the literature.[46] We duly note, however, that the charging characteristics of the interface are sensitive to various experimental parameters and so resorting to literature values does limit the accuracy of the method. Our point here, however, is to show the general value of the electrocapillary approach, and so literature values readily suffice. In using such data for our specific system, we assume that the charge on the gold−liquid surface is zero at the E_{PZC}^{GL}, which is a good assumption for a $KClO_4$ solution (no specific adsorption).

Electrocapillary Approach Applied to Direct Adhesion Measurements. In Figure 5 we plot the work of adhesion with applied potential. The dashed lines correspond to predictions from the electrocapillary approach as given by eq 7. We consider the PZC and the PZF to both physically represent the applied potential at which no charge is accumulated on the surface. Literature data provide us with the PZC, and our double layer measurements allow us to extract the PZF. Therefore, the potential axis in Figure 5, ΔE, represents the potential away from zero charge (where the PZC is defined as E_{PZC}^{GL} for the model predictions and E_{PZF} for our experimental data).

As previously stated, fitting the experimental data to the theory provides a framework for estimating the charge density at the gold−mica interface as shown in Figure 6a. The charge at the gold−mica interface is obtained from eq 5 using the parameters obtained from fitting the experimental data. We observed little dependence on concentration so only the charge corresponding to 10^{-3} M is used. The analysis reveals that the magnitude of the charge at the gold−mica interface is comparable to that of the charge at the gold−liquid interface. The high charge developed in the contact region is of similar strength to the charge of the mercury−mica interface, as estimated by Horn et al.[45] using a similar theoretical framework.

An especially elegant result of the electrocapillary approach is a direct (parameter-free) prediction of the charge difference between the gold−liquid and the gold−mica interfaces. This follows directly from the definition of work of adhesion:

$$\left(\frac{\partial W_{ADH}}{\partial E}\right)_{P,T,n_i} = \left(\frac{\partial \gamma_{GL}}{\partial E}\right)_{P,T,n_i} + \left(\frac{\partial \gamma_{ML}}{\partial E}\right)_{P,T,n_i} - \left(\frac{\partial \gamma_{GM}}{\partial E}\right) = \sigma_{GM} - \sigma_{GL} = \Delta\sigma \quad (8)$$

Figure 6b shows the calculated charge difference between the gold−liquid and gold−mica interfaces for different concentrations. (Values were obtained by differentiating a polynomial fit to the measured adhesion.) The analysis shows that the charge at the gold−mica interface is always greater than the charge at the gold−liquid interface. The electrocapillary approach is simple and very intuitive, and its use underscores the relationship between the different components of the work of adhesion, especially between the gold−liquid and the gold−mica surface energies.

Conclusion

We have measured double layer forces and adhesion between a gold electrode and a mica surface as the electric potential of the gold surface was changed. The observed double layer repulsion was well represented by DLVO theory at long range but showed strong deviations from the predictions at short range. We also observed a PZF of around 0.25 V versus Ag/AgCl(3M). We showed that the work of adhesion (measured from pull-off forces) depends strongly on the applied potential and proposed that the dependence of adhesion on potential is due to potential-dependent charging at the gold−mica interface. To analyze these data, we developed a simple model based on electrocapillarity that predicts the dependence of adhesion on the applied potential. Using this approach, we demonstrated that the charge of the gold−mica interface is larger than the charge of the gold−liquid interface. This framework is not only applicable to surface force measurements but could also be of use in the development of microfluidic devices designed on the concept of electrocapillarity, such as those of Lee and Kim,[2] and may be valuable in the design of components (switches, gates, etc.) for aqueous-based MEMS.

Acknowledgment. This work was funded through National Science Foundation via the Materials Research Science and Engineering program Grant DMR 0213706 and also by the NSF Grant CTS-9907687

LA047750X

(46) Amokrane, S.; Badiali, J. P. *J. Electroanal. Chem.* **1989**, *266*, 21.